LA-5826-MS
Informal Report

UC-38
Reporting Date: December 1974
Issued: January 1975

Characterization of Rock Melts and Glasses Formed by Earth-Melting Subterrenes

by

L. B. Lundberg

los alamos
scientific laboratory
of the University of California
LOS ALAMOS, NEW MEXICO 87544

UNITED STATES
ATOMIC ENERGY COMMISSION
CONTRACT W-7405-ENG. 36

In the interest of prompt distribution, this LAMS report was not edited by the Technical Information staff.

Work partially supported by a grant from the National Science Foundation, Research Applied to National Needs (RANN).

Printed in the United States of America. Available from
National Technical Information Service
U.S. Department of Commerce
5285 Port Royal Road
Springfield, VA 22151
Price: Printed Copy $4.00 Microfiche $2.25

CHARACTERIZATION OF ROCK MELTS AND GLASSES FORMED BY EARTH-MELTING SUBTERRENES

by

L. B. Lundberg

ABSTRACT

Rock melts and glasses formed by earth-melting Subterrenes have been studied in some detail. Data are presented on both the molten and the solid rock-glass products formed. The melting behavior, thermal transport, viscosity, electrical resistivity, and solidification behavior of several molten rock-glasses are described. The visual appearance, gas and water permeabilities, thermal expansion, thermal conductivity, and crush strength of several solid rock-glasses are also documented.

I. INTRODUCTION

The penetration of the earth by melting, with subsequent reforming of soils and rocks into useful shapes, is a major advantage of Subterrene devices.[1] These devices are designed to:

- form holes in geologic formations,
- remove excess material, and
- leave a self-supporting hole lining in a single operation.

Most rocks and soils can be fused at high temperatures (1400 to 2200 K); and, because their major constituent in most cases is silica (SiO_2), the melts formed during heating and the solids formed during cooling can be compared to silicate glasses. However, the usual operating conditions of Subterrene devices generally do not form uniform glasses. Rocks and soils are mostly complex mixtures of oxides, which have been formed into solid solutions, minerals, or glasses. When these mixtures are heated, the lower melting phases begin to flow and mix with the remaining solid material. When the average viscosity of the melt becomes low enough, the mixture flows out of the path of the penetrator and is deposited either on the hole wall or is channeled into a debris-removal system. Although the process of melting rocks and soils with the Subterrene system has been discussed in some detail before,[2] we will present herein an additional discussion of the melting process along with some data on the properties of the glassy solid products formed during rock penetration.

II. MOLTEN ROCK

The properties of the molten rock or soil have a significant effect on the performance of a Subterrene penetrator. The penetrator tip must raise the temperature of the surrounding medium sufficiently to make it flow. To design a melting penetrator, one needs to consider, e.g., the melting behavior of the medium, the transport of heat to it and through it, the viscosity of the resulting melt, and the solidification of the melt. These properties have been studied for some rocks and soils in experimental work that investigated their melting behavior, the viscosity and its electrical resistivity of the melt.

A. Melting Behavior

The melting behavior of rocks and soils was studied in a Leitz high-temperature microscope stage. A sample of the rock or soil was placed in a small tantalum crucible set on a tantalum strip that was heated by passing an electrical current

through it. The microscope stage was located inside a gas-tight chamber which was evacuated and back-filled with argon prior to heating the specimen. The specimen was viewed through a quartz window. An optical pyrometer measured the temperature in the tantalum crucible to about ± 20 K.

The melting behavior of twelve different samples was studied in this apparatus. A summary of the data is given in Table I.

In general, rocks and soils melt inhomogeneously, with some gas evolution usually observed. The inhomogeneous melting is caused by the fact that rocks and soils are generally made up of a mixture of solid phases (also gases and liquids) each of which may or may not have a discrete melting point. Some rocks and most soils are so inhomogeneous that they show a very wide melting range plus large changes in the melt properties during the melting process. Bandelier tuff, for example, starts out the melting process by forming a very fluid liquid containing rather large quartz (SiO_2) crystals. A photomicrograph of unmelted Bandelier tuff is seen in Fig. 1. As the melting progresses, the liquid starts to dissolve the quartz crystals and the viscosity is seen to increase. Of course, gas is evolving from the rock during heatup causing the melt to froth continually (if not pressurized).

Some rocks do not melt in the normal sense. As pointed out by Krupka,[5] limestones diminish in their propensity to melt as the calcite content increases. In an open system, calcite ($CaCO_3$) decomposes to a high-melting (2840 K) compound, calcium oxide (CaO) and carbon-dioxide gas (CO_2). Naturally occurring minor constituents in limestone, such as water and silica, tend to improve the situation with regard to melting. Water, for example, added to calcite in a closed system can reduce the minimum pressure and temperature conditions for melting from 4 MPa and 1500 K[4,5] to 1 MPa and 920 K.[6,7] Silica and calcite mix chemically to form phases with significantly reduced melting temperatures. For instance, the lowest melting eutectic in the $CaSiO_3$-SiO_2 system melts at 1710 K.[8]

TABLE 1

MELTING BEHAVIOR DATA

Material	Melting Temperatures, K Start	Complete	Remarks
Bandelier tuff	---	1750	Melt viscosity increased as quartz crystals were consumed.
Jemez basalt-1[a]	---	1570	Melts uniformly with some gas evolution.
Jemez basalt-2[b]	---	1510	
Bresser basalt	---	1570	
Charcoal granite[c]	---	1670	Dark phase melted first and then proceeded to consume the matrix.
Westerly granite	---	1760	
Sioux quartzite	---	1760	
Tennessee ping marble	---	--	Heated to 2270 K without melting, some decomposition.
Shale, Santa Fe County, New Mexico	1470	1560	Discrete phase melting accompanied by gas evolution. Viscosity increased as more material melted.
Caliche, Santa Fe County, New Mexico	1570	1850	
Green River Shale, Cuba, New Mexico	1550	1600	
Concrete	1620	1700	Localized melting. Less gas evolution than from shales or caliche.
Coal, Madrid, New Mexico	---	--	Heated to 2120 K without signs of melting.

[a]Started with rock fragments ~ 1 to 3 mm.

[b]Started with powder ≲ 1 mm.

[c]Also called St. Cloud gray granodiorite.

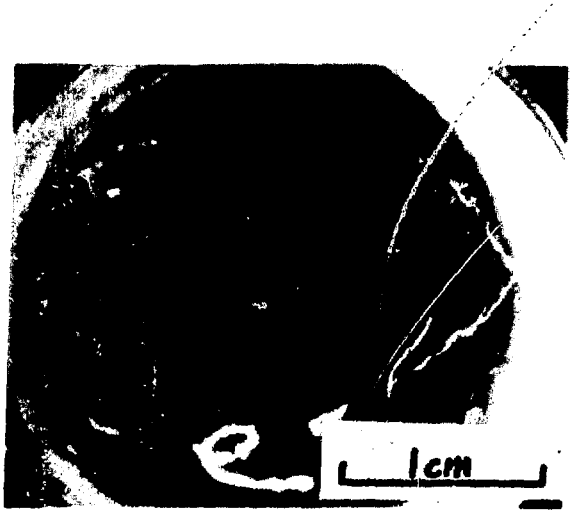

Fig. 1. Bandelier tuff. Transparent inclusions are quartz crystals.

B. Thermal Transport

The transport of heat through the molten rock is a process fundamental to the operation of a Subterrene device. Heat energy is transferred into the rock to fuse it and out of the melt to solidify it. The process of transferring heat from the penetrator to the rock is complicated. Because the melt is forming the leading surfaces of the penetrator, there are problems of heat-coupling between the penetrator and the rock. These problems arise from, e.g., rock-surface irregularities, gas evolution during melting, and solid particles in the melt. As the melt passes toward the aft areas of a penetrator, the melt becomes more uniform and starts to behave like a molten glass. These melt characteristics plus the pressures built up in the melt tend to reduce the coupling problems as the melt is moved toward the aft regions of the penetrator. The transfer of heat through a uniform glass is a complicated process (e.g., Ref. 9), because it involves both radiation and "true" conduction. The heat-flow phenomena on the exterior aft section of the penetrator are similar to those encountered in machine-forming of glass containers, which has been studied.[10]

A critical review has been made at LASL of the heat-transfer behavior of rocks and rock melts.[11] In rocks and rock melts, as in glasses, thermal conductivity is not a fundamental property so that an "apparent conductivity" is measured in a steady-state heat-flow experiment. Data from this type experiment are affected by thickness and other experimental details. The shape of the temperature-vs-thermal conductivity curves in Fig. 2 is typical for rock materials. These curves demonstrate that a smooth transition from one heat-transfer process to another in rocks does not generally occur, as it does in a silica glass (see Curve 3, Fig. 2).

The basalt is completely molten above 1550 K, and it starts to melt at ≈ 1320 K.[13] This change of state causes the inflection point in the thermal conductivity-temperature relationship. The inflection point seen in Curve 3 does not correspond to complete melting, but probably represents the initiation of partial melting to a glass material distributed in such fashion as to cause a radical change in the internal boundaries, i.e., it causes the material to transmit significant quantities of radiant energy.

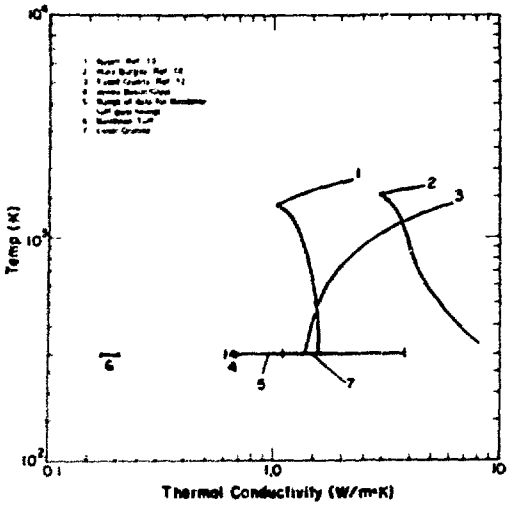

Fig. 2. Thermal conductivity of rocks and glasses.

The complexity of the heat transfer to and through the molten glass formed during rock-melting suggests that the fundamental thermophysical properties of these materials would be difficult, at best, to utilize in an analytical treatment of a Subterrene penetrating rock. Thus, McFarland's[15] model for heat transfer from a penetrator must be compared extensively with experimental data before its utility can be assessed.

C. Viscosity

For a Subterrene device to penetrate rock or soil, the melt formed must flow under modest pressure. In general, the melt should be no more viscous than commerical glass which is normally worked below a viscosity of 10^3 Pa·s.[16] A typical Subterrene operating envelope, based on this viscosity criterion and the practical temperature limitations of a pure molybdenum penetrator, is defined in Fig. 3. This figure also illustrates the fact that the viscosities of rock and glass melts are highly temperature dependent: a small increase in temperature can cause them to be much more easily worked, i.e., more easily penetrated with a Subterrene device. The viscosities, η, of both glass and rock melts follow a temperature-dependence relationship of the form:

$$\eta = A \exp Q/T,$$

where A and Q are approximately constant for a given rock or glass. Note in Fig. 3 that the activation energies, Q, for viscous flow of silica glasses and siliceous rocks are similar, whereas there are large differences in the frequency factor, A.

A contradiction between theory and practice is illustrated in Fig. 3 in that the viscosity measured for Bandelier tuff-glass indicates it cannot be penetrated with a molybdenum penetrator, which is contrary to both laboratory and field experience. The explanation of this phenomenon lies in the fact that, as pointed out earlier, Bandelier tuff is quite inhomogeneous and the first-melting materials yield a highly fluid liquid. The viscosity data presented in Fig. 3 are for tuff that had been heated 4 h in air at 1720 K.

Figure 3 also illustrates that some natural geologic materials cannot be easily penetrated with a Subterrene device even when the temperature is raised very high. For example, even if the device would raise pure Cristobalite quartz to its melting point, 1980 K, the viscosity at this temperature is well over 10^6 Pa·s. In such cases, the only other alternative is to consider fluxing agents. A few preliminary experiments were performed with B_2O_3 as a flux for Bandelier tuff-glass because this compound has relatively low viscosity (see Fig. 3) and is readily miscible with silica. The experiments involved placing B_2O_3 powder on the surface of a tuff-glass hole lining and heating with an oxyhydrogen torch. A new glass formed quite readily, and it had a viscosity much lower than the parent rock-glass.

Viscosity data were also obtained for Jemez and Presser basalts at Corning Glass Works as a function of temperature over the temperature range 1390 to 1790 K. The data were obtained by rotational viscometry methods described in the appendix. These data are compared with published data for molten basalt in Fig. 4. Note that the published data show a break in the log η-vs-1/T curve at ~ 1500 K, whereas the present data exhibit no such break. This difference is believed to be caused by supercooling of the melts in the present work. In other words,

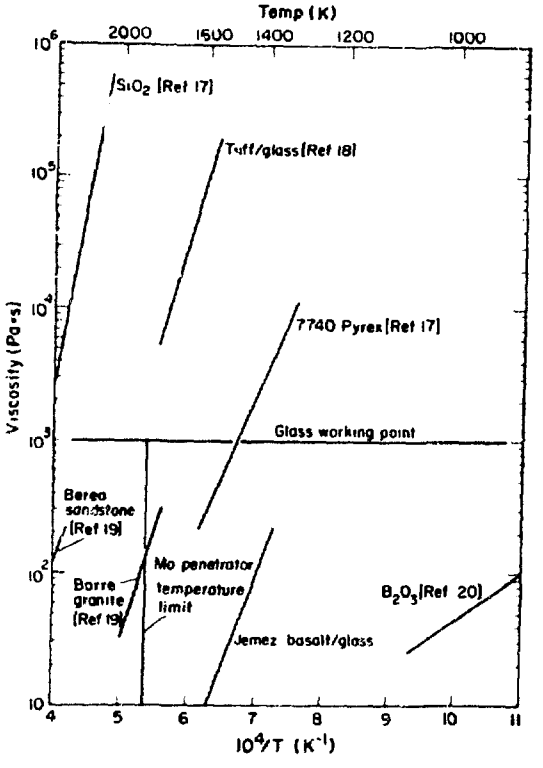

Fig. 3. Viscosity of glasses and rock-glasses.

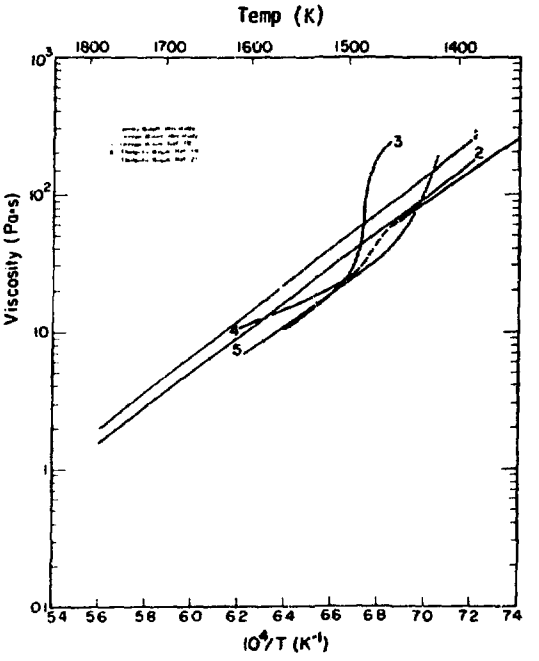

Fig. 4. Variation of basalt viscosity with temperature in the melting range.

crystallization was suppressed, and the glass state was maintained to a lower-than-normal temperature. The equations that best describe the data from the present study are, for Jemez basalt,

$$\eta \text{ (Pa·s)} = 9.95 \times 10^{-8} \exp (30000/T)$$

and, for Dresser basalt,

$$\eta \text{ (Pa·s)} = 1.01^{-7} \exp (29600/T).$$

The viscosity data for homogeneous rock or soil melts should be used with caution in analyzing penetrator performance primarily because, in the operational situation, the melt contains both gas bubbles and solid particles. Analysis of the real problem should include the effects of these inhomogeneities (see for example Refs. 21 and 23), at least in an exploratory fashion to determine whether the penetrator performance predictions are significantly affected.

D. Electrical Resistivity

Electrical resistivity data on molten rocks and soils are especially important to advanced Subterrene concepts which involve electrical self-heating of the melt. This glass-heating process is found in the Pochet furnace used in glass manufacture.[24] Bacon's[19] data for nine different rock types indicate that molten rocks (see Fig. 5) have resistivities in the semiconducting range (0.01 to 10 Ω·m) and that they behave like molten electrolytes.[25]

We have obtained experimental data on electrical resistivity of molten Jemez and Dresser basalts over the temperature range 1390 to 1790 K simultaneously with the viscosity data using the experimental methods described in the Appendix. The temperature dependence of electrical resistivity, ρ, of molten rocks is of the same form as for viscosity. The equation that best fits the data from this study for Jemez basalt is

$$\rho \text{ (Ω·m} = 4.87 \times 10^{-2} \exp (18200/T);$$

and for Dresser basalt,

$$\rho = 2.28 \times 10^{-2} \exp (19100/T).$$

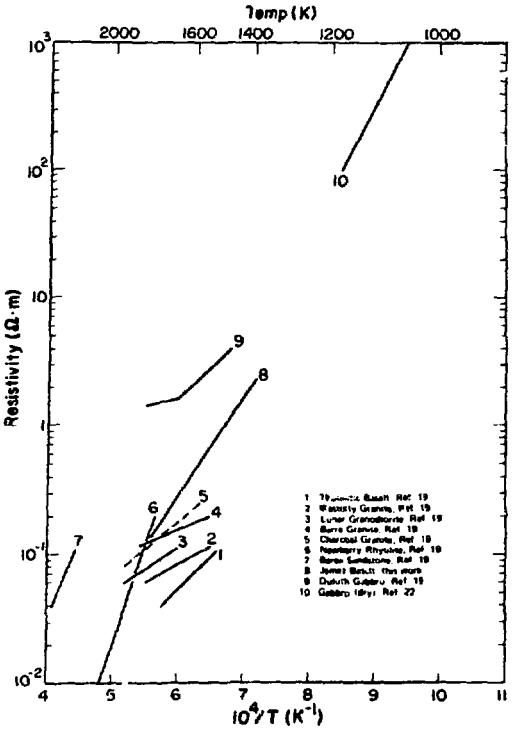

Fig. 5. Electrical resistivity of rock as a function of temperature.

The electrical-resistivity data obtained in this study have been converted to conductivity and plotted in Fig. 6 for comparison with other data for basalt. This figure reveals the rather large variations in the conductivity of basalts. However the least variation is found in the molten state. The large variation at lower temperatures, in the solid state, is caused to a large extent by the degree of crystallinity.

Presnall[26] has demonstrated the effect of the amount of crystallinity very convincingly by plotting the conductivity change of a crystalline basalt with increasing temperature (lower curve, Fig. 6) and comparing changes with the behavior at decreasing temperature (upper curve). In the cooling case, the basalt does not completely recrystallize during the experiment. The breaks seen in Presnall's cooling curve and in Curves 1, 2, and 4 are near the temperatures at which we observed crystallization in the two basalts we investigated: 1331 K for Dresser basalt and 1318 K for Jemez basalt.

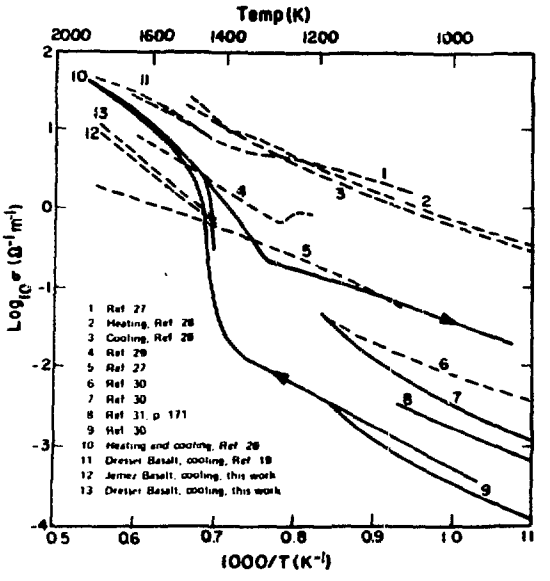

Fig. 6. Comparison of electrical conductivity data for liquid, glassy, and crystalline basalts at 1-atm pressure.

Figure 6 also indicates the variation of electrical conductivity with the experimental conditions. Note a rather large variation between our data for Dresser basalt and the data published by Bacon et al.[19] The major difference between the two experimental methods is in the atmosphere over the melt during the measurements. Bacon's data were obtained in argon whereas we obtained our data in air. Because molten basalt behaves like an electrolyte, the ionic motion, which governs the conductivity, will be affected by the oxidation state of the ions. This oxidation state is governed by the atmosphere over the melt.

I. Rock-Glass Solidification

The molten material formed by a Subterrene is generally either pressed against the wall of the borehole and/or passed through a central opening in the penetrator for eventual removal from the hole. In either case the melt is generally cooled rapidly enough to form a glassy solid which, as pointed out earlier, usually contains gas bubbles and crystalline particles.

The problem of melt cooling and solidification on the borehole has been modeled on the computer for 50- and 75-mm-diam consolidating penetrators.[32] In our study we found that the cooling is strongly affected by penetrator afterbody and stem design, which indicates that controlled cooling of a borehole lining (to minimize residual stresses in the glass) could be achieved by design. Experimental data are compared in Fig. 7 with the numerical results for a 75-mm penetrator in Bandelier tuff. The "effective" thermal conductivity, λ, used for the rock is seen to influence the analysis significantly, which indicates that accurate thermal-property data for the rock being penetrated are needed if we wish to predict the cooling rate of the borehole lining

III. SOLID ROCK-GLASS

The glassy solid bodies formed by a Subterrene fall into two categories:

- hole linings, and
- hole debris,

both of which have useful properties. The properties of the hole linings studied include:

- visual appearance,
- gas and water permeabilities,
- thermal conductivity, and
- crush strength.

Only visual examinations have been made on hole debris.

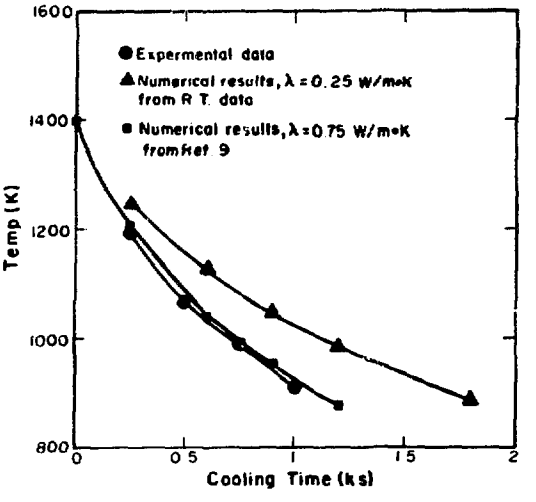

Fig. 7. Comparison of experimental temperature data with results from computer analyses. 75-mm penetrator in tuff.

A. Visual Appearance

The hole linings in loose formations are especially useful in preventing cave-ins immediately after removal of the hole former. A typical hole lining made in Green River shale rubble with a consolidator penetrator is seen in Fig. 8. This hole lining was simply dug out of the surrounding rubble; it had sufficient structural integrity to be handled without excessive care. To be sure, the hole lining contains many defects, such as cracks and voids (both closed and open), but, as illustrated in the figure, it is structurally much sounder than the parent formation.

A typical cross-sectional view of a longitudinal section of a hole lining is shown in Fig. 9(a). Bandelier tuff is, petrologically, an aggregate of rhyolitic ash, quartz crystals, and feldspars (see Fig. 1), and the hole lining is also an aggregate consisting of a glassy matrix that contains partially melted quartz crystals and feldspars. The dark streaks in the lining are melted, unmixed, dark-colored minerals which were deposited during hole formation. These streaks delineate the flow pattern around a moving penetrator. The radial cracks in this hole lining have resulted from tensile stresses built up during cooling by axial shrinkage relative to the parent rock. Some radial cracks are also caused by circumferential thermal stresses. The hole lining in tuff, Fig. 9(a), does not have very many bubble defects as compared to the lining in Green River shale, Fig. 8.

If Bandelier tuff is heated to a high enough temperature and held for a sufficient length of time, it will form a green-colored, transparent glass. The sample seen in Fig. 9(b) was prepared by heating the tuff under an inert atmosphere in a molybdenum crucible at 2100 K for 11 ks. It will be noticed in the photograph, Fig. 9(a), that no quartz crystals remain.

These glass linings generally adhere quite well to the rock; they can be, and usually are, held to a high overall diametral dimensional tolerance. For example, 51-mm-diam holes are typically held to ± 127 μm over extended lengths.

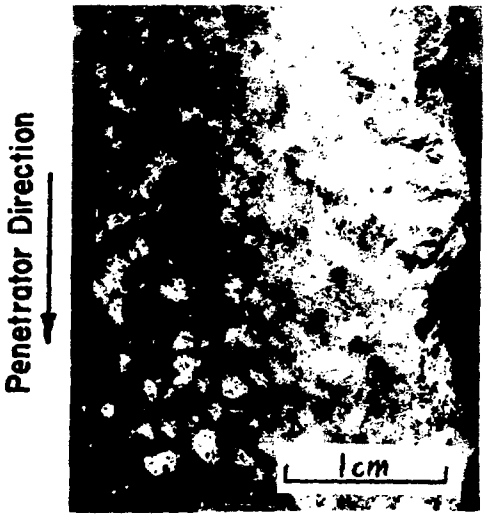

Fig. 9(a). Hole lining formed in Bandelier tuff.

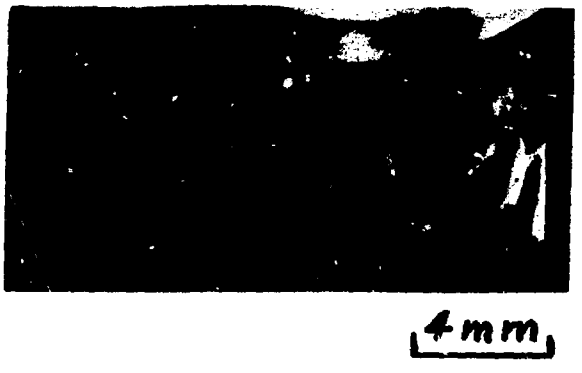

Fig. 9(b). Equilibrium glass formed from Bandelier tuff.

Fig. 8. Hole formed by Subterrene in Green River shale rubble.

The debris that must be removed from holes in hard rock is generally a glassy product. Some shapes the debris takes are shown in Fig. 10. This material was removed from the borehole by passing the molten rock up through a central hole in the penetrator where the liquid was struck by a high-velocity gas flow that both solidified the melt and lifted the debris from the hole. The high-velocity gas flow causes the rock glass to form into products ranging from porous glass particles to glass fibers (see Fig. 10).

B. Gas and Water Permeabilities

Gas permeability data (N_2 flow at 0.5 atm) for various rock formations are given in Table II. These data were derived from small samples, cubes ~ 1.3 cm on a side. Although much more permeable than dense granite, the glass is several orders of magnitude tighter than the parent tuff.

For comparison we conducted a water permeability experiment on a rotary drilled 51-mm-diam hole in tuff and on a glass-lined Subterrene hole of the same size melted in the same material. The bottoms of the holes were sealed off. The results of this test are shown in Fig. 11. The 0.36-m-deep holes were filled with water and the times to flow radially out under the gravity head into the tuff were recorded by observing the sinking water level. Note that seepage of water through the glass lining of

TABLE II

GAS PERMEABILITIES OF NITROGEN FLOW AT 0.5-atm PRESSURE

Material	Permeability, 10^3 Darcy[a]
Bandelier tuff	243.0
Bandelier tuff glass	8.0
Jemez basalt	0.5 - 10.0[b]
Jemez basalt-glass	Not detectable
Dense granite	0.3

[a] The American Petroleum Institute defines a Darcy as follows: "A porous medium has a permeability of one Darcy when a single phase fluid of one centipoise viscosity that completely fills the voids of the medium will flow through it under conditions of viscous flow at the rate of one cubic centimeter per second per square centimeter under a pressure equivalent hydraulic gradient of one atmosphere per centimeter."

[b] Wide variation due to rock variability.

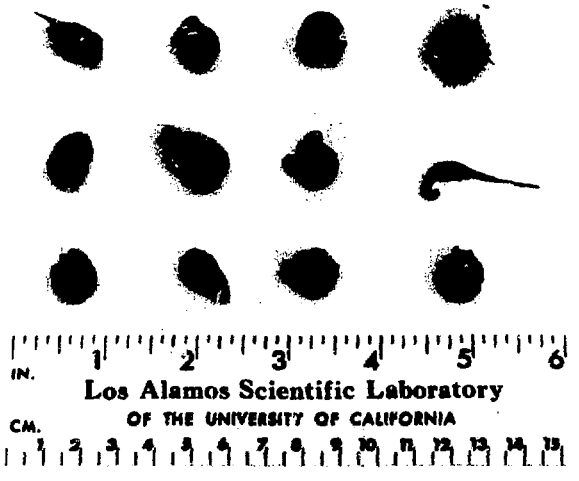

Fig. 10. Debris from holes in hard rock.

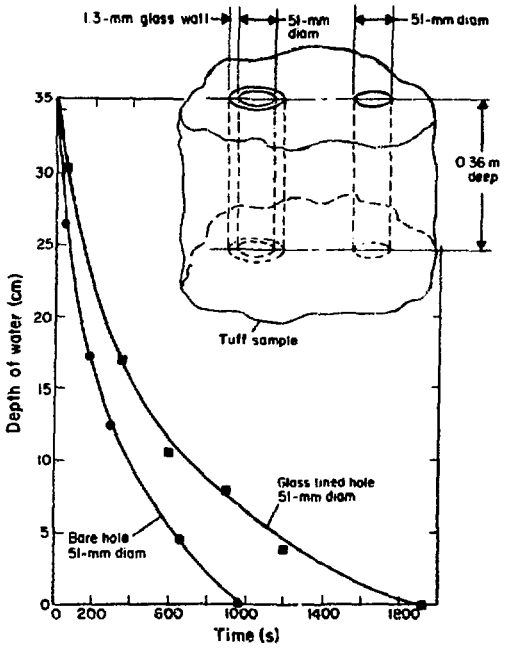

Fig. 11. Comparison of water drainage rate from glass-lined and bare holes in Bandelier tuff.

the hole, even though the lining had cracks and chill-wrinkles, was still only half as fast as through natural tuff. Water outflow from the glass-lined hole was through fine thermal-stress cracks and through other gross defects. True sealing of the hole would require elimination of these defects.

C. Crush Strength

Crush-strength data on unconstrained samples were obtained for rocks and rock-glasses to determine their relative compressive strengths. Jemez basalt and a uniform Jemez basalt-glass prepared at Corning Glass Works by melting the rock in a platinum crucible in air for 4 h at 1720 K were tested. Also, Bandelier tuff and Bandelier tuff glass taken from hole linings made by two different penetrators were tested. Three dried Bandelier tuff samples cut into rectangular parallelepipeds measuring 25 by 50 by 50 mm were also tested. All other samples were cut into cubes 13 mm on a side. The crush tests were performed on an Instron test machine. Cardboard pads were placed between the load platens and the specimens to reduce the error in strength measurement caused by sample end friction.

The crush-test data are listed in Table III. Note that the tuff-glass specimens were loaded in directions corresponding to their orientation in the hole wall. There appears to be a significant difference in crush strength of tuff-glass from the wall of the 51-mm-diam hole, depending on direction of loading, but not in the specimens taken from the wall of the 114-mm-diam hole. There is only a slight variation in crush strength with density for the tuff-glass from the 114-mm-diam hole. The major differences occur between the parent rock and the rock-glass. For tuff, the rock-glass is as much as 50 times stronger than the parent rock. The tuff-glass from the 114-mm hole was stronger than from the 51-mm hole because the lining from the former hole was thicker and more uniform.

From a structural standpoint, the rock-glass in a hole lining in general resembles a competent rock more closely than a uniform glass. High strengths could be easily obtained by reducing gross defects in the rock-glass such as cracks and bubbles. Obviously, penetrator design and operation affect the strength of the hole lining too.

TABLE III

CRUSH STRENGTH OF ROCKS AND ROCK-GLASSES

Material	Crush Strength, MPa	Number of Specimens
Jemez basalt	44^{+46}_{-26}	10
Jemez basalt-glass[a]	108^{+101}_{-72}	4
Bandelier tuff	$2.8^{+0.3}_{-0.5}$	3
Bandelier tuff-glass from 51-mm-diam-hole wall		
Axial	55^{+58}_{-23}	5
Tangential	36^{+3}_{-3}	2
Bandelier tuff-glass from 114-mm-diam-hole wall		
Axial (2.3 Mg/m^3)	126^{+37}_{-23}	4
Axial (2.2 Mg/m^3)	110^{+8}_{-12}	3
Radial (2.3 Mg/m^3)	115^{+14}_{-16}	3
Tangential (2.3 Mg/m^3)	132^{+27}_{-42}	3

[a] Uniform glass prepared by Corning Glass Works.

D. Glass Thermal Expansion

Corning Glass Works measured the thermal expansion of a uniform Jemez basalt-glass over the temperature range 293 to 573 K. The mean linear coefficient of thermal expansion over this temperature range was 6.9×10^{-6} K^{-1}. This value is intermediate in the range of expansion coefficients for commercial glasses (see, for example, Ref. 16).

E. Thermal Conductivity

The room-temperature (303 K) thermal conductivity of Bandelier tuff, Bandelier tuff-glass, Jemez basalt-glass, and a local granite has been measured. The rock samples were 25-mm-diam by 6-mm-high right-circular cylinders and were measured in a

steady-state, comparison device operating with a 100 to 200 K/m temperature gradient. The rock-glass samples were 1-cm cubes and were measured in a probe device. The tuff-glass was taken from a hole lining, whereas Jemez basalt-glass was prepared by Corning Glass Works by heating in air at 1720 K for 4 h. The data, listed in Table IV, show rather large variations due primarily to the nonuniformity of the materials. These data are plotted in Fig. 2 for comparison with published data on rocks and glasses. Note that the room-temperature thermal conductivities of the dense local granite and of the rock-glasses are comparable to the published data for dense rock and glass. The tuff has much lower thermal conductivity because of its high porosity.

IV. SUMMARY AND CONCLUSIONS

A broad, cursory characterization of rock-glass has been made. Samples from both Subterrene penetrations and from laboratory-prepared melts have been studied.

The melting behavior of rocks and soils was studied experimentally and was found to be quite dependent upon the homogeneity of the starting material. Rocks and soils, in general, melt inhomogeneously with gas evolution and changing melt properties as fusion proceeds.

Heat conduction into and through rock, rock melts, and solid rock-glasses was studied primarily from a theoretical standpoint; only a few room-temperature experiments were performed. From literature studies it was seen that thermal transport in molten rock is comparable to that in glass, i.e., a large fraction of the heat is transferred by radiation.

TABLE IV

ROCK AND ROCK-GLASS THERMAL CONDUCTIVITY DATA

Material	Thermal Conductivity (λ) W/m·K
Bandelier tuff	0.17 to 0.21
Bandelier tuff-glass	0.6 to 1.1
Jemez basalt-glass	0.67
Local granite	1.1 to 3.8

Viscosity and electrical resistivity of molten rocks were measured as a function of temperature. Molten Dresser and Jemez basalts had viscosities of $\sim$ 200 Pa·s at 1390 K and 2 Pa·s at 1790 K, respectively, whereas their resistivities were $\approx$ 2 Ω·m at 1390 K and 0.1 Ω·m at 1790 K. The measured viscosity of Bandelier tuff did not correlate too well with the performance of a penetrator.

Rock-glass solidification in a borehole was examined analytically to determine whether rock-glass cooling rates could be predicted. We concluded that the cooling rates and subsequent thermal stresses could be predicted reliably if accurate rock thermal-property data were available.

The visual appearances of typical solid rock-glass products formed by Subterrene penetrators were discussed in detail.

Gas and water permeabilities of glass-lined holes were measured and were substantially lower than for the parent rocks.

Crush strengths of tuff-glass and basalt-glass borehole lining samples were measured and compared with the crush strength of the parent rock. As might be expected, the rock-glasses were much stronger.

The thermal-expansion behavior of Jemez basalt-glass was measured to be 6.9 x 10^{-6} K^{-1}, which is comparable to that of some commercial glasses.

Room-temperature thermal conductivities of several rocks and rock-glasses were measured. The data were consistent with published values.

ACKNOWLEDGMENTS

The author wishes to express his gratitude to those LASL personnel who made significant contributions of their time and talent to this work. These people include C. G. Hoffman, who performed most of the micrography; C. A. Javorsky, who performed the hot-stage microscopy; and W. L. Sibbitt, who performed the thermal conductivity measurements. A special thanks goes to J. C. Rowley, who supplied the stimulus for this work plus a significant fraction of the data.

APPENDIX

ROCK VISCOSITY AND ELECTRICAL RESISTIVITY EXPERIMENTAL METHODS AND RESULTS

The viscosity and electrical resistivity as a function of temperature were measured simultaneously in the same apparatus at Corning Glass Works, Corning, NY. The apparatus is very similar to that used by Babcock[33] to measure the viscosity and electrical conductivity of molten glasses.

Basically, the apparatus consists of a rotational concentric-cylinder viscometer[34] with a platinum cup and spindle (inner cylinder). The measurements were made in air in a platinum-wound electric furnace. Starting from the highest temperature and working downward, the temperature was stabilized before each viscosity and electrical-resistivity measurement. The temperature of the melt was measured with a thermocouple located inside the spindle. The viscosity data were derived from the torque imparted to the spindle when the cup was rotated at a constant velocity. The electrical-resistivity data were derived from ac (1 kHz) resistance between the spindle and the cup. Alternating current is required for the resistivity measurements because molten basalt is a liquid electrolyte and would become polarized in a steady electric field. The resistance was measured with a General Radio Type 1650-A portable impedance bridge. Measurements of both properties were made in the range of 1390 to 1790 K. The rock used for the measurements had been crushed and heated at 1823 K for 2.5 h in air in the platinum crucibles used in the viscometer. The heat was supplied by an electric furnace. The premelting yielded a black, opaque, uniform glass. X-ray diffraction indicated the product was noncrystalline. The chemical composition of the rocks and rock-glasses are listed in Table A-1. The viscosity and resistivity data are tabulated and plotted in Figs. A-1 through A-4.

TABLE A-1
CHEMICAL COMPOSITION OF ROCKS AND ROCK-GLASS

	Composition, wt%			
Constituents	Dresser Basalt	Dresser Basalt-Glass	Jemez Basalt	Jemez Basalt-Glass
SiO_2	48.2	49.52	50.01	50.09
Al_2O_3	16.13	15.54	16.82	16.81
Fe_2O_3	7.65	8.19	2.83	4.38
FeO	5.41	4.68	7.60	6.53
MgO	6.25	6.50	6.70	6.69
CaO	8.69	10.05	9.62	9.68
Na_2O	2.54	2.47	3.94	3.40
K_2O	0.96	0.97	0.97	0.94
H_2O	0.38	0.004	0.14	0.003
TiO_2	1.45	1.66	1.38	1.46
P_2O_5	0.16	--	--	--
CO_2	0.048	0.003	0.02	0.003
B_2O_3	--	--	--	--
MnO	--	0.18	0.15	0.15

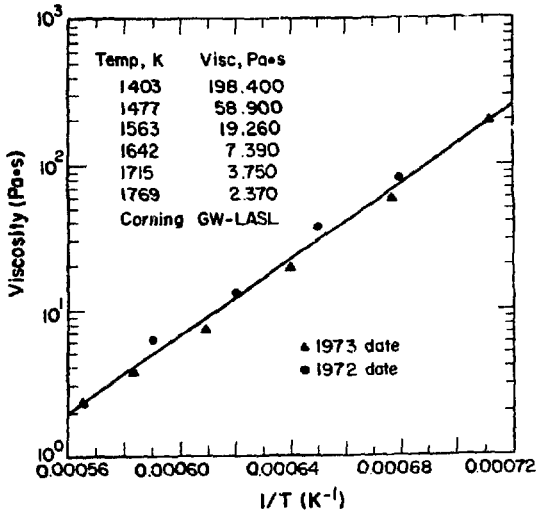

Fig. A-1. Molten Jemez basalt viscosity.

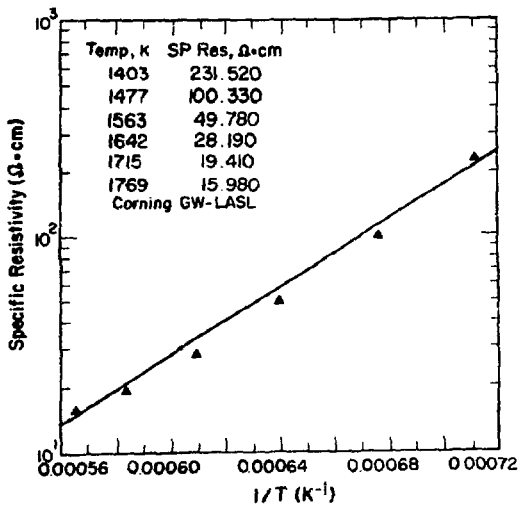

Fig. A-2. Molten Jemez basalt resistivity.

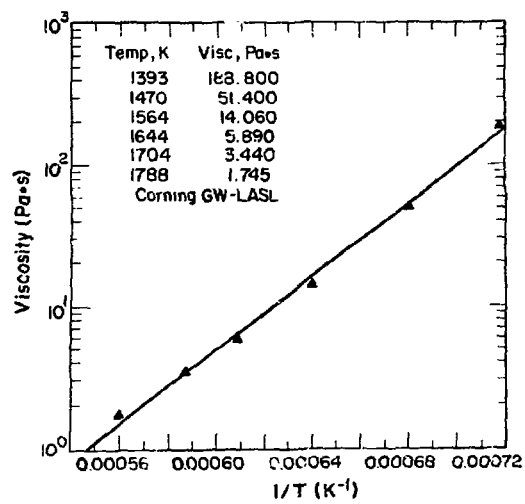

Fig. A-3. Molten Dresser basalt viscosity.

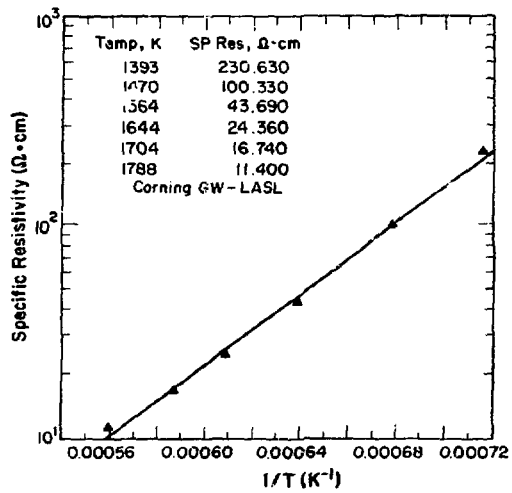

Fig. A-4. Molten Dresser basalt resistivity.

REFERENCES

1. M. C. Smith, Ed., "A Preliminary Study of the Nuclear Subterrene," Los Alamos Scientific Laboratory Report LA-4547 (April 1971).

2. M. C. Krupka, "Phenomena Associated with the Process of Rock Melting. Application to the Subterrene System," Los Alamos Scientific Laboratory Report LA-5208-MS (February 1973).

3. M. C. Krupka, LASL, Private Communication, January 1972.

4. F. H. Smyth and L. H. Adams, J. Am. Chem. Soc. 45, 1167 (1923).

5. E. H. Baker, J. Chem. Soc. 464 (1962).

6. P. J. Wyllie and O. F. Tuttle, J. Petrol. 1, 1 (1960).

7. P. J. Wyllie and E. J. Raynor, Am. Mineralogist 50, 2077 (1965).

8. M. K. Reser, Ed., "Phase Diagrams for Ceramists," Am. Ceram. Soc., (1964); Supplement (1969).

9. E. A. Anderson and R. Viskanta, "Effective Thermal Conductivity for Heat Transfer Through Semitransparent Solids," J. Am. Ceram. Soc. 56, 541 (1973).

10. D. A. McGraw, "Transfer of Heat in Glass During Forming," J. Amer. Ceram. Soc. 44, 353-363 (1961).

11. W. L. Sibbitt, LASL, Private Communication, January 1974.

12. R. W. Powell, C. Y. Ho and P. E. Liley, "Thermal Conductivity of Selected Materials," US-NBS report NSRDS-NBS 8 (1966).

13. T. Murase and A. R. McBirney, "Thermal Conductivity of Lunar and Terrestrial Igneous Rocks in Their Melting Range," Science 170, 165-167 (1970).

14. K. Kawada, "Variation of Thermal Conductivity of Rocks, Pt. 2, Bull. of the Earthquake Res. Inst. 44, 1071-1091 (1966).

15. R. D. McFarland, "Numerical Solution of Melt Flow and Thermal Energy Transfer for the Lithothermodynamics of a Rock-Melting Penetrator," Los Alamos Scientific Laboratory Report LA-5608-MS (May 1974).

16. J. R. Hutchins, III and R. V. Harrington, "Glass," Encyclopedia of Chemical Technology, 2nd Edition, Vol. 10, Kirk-Othmer (Ed.), John Wiley & Sons, pp. 533-604.

17. J. F. Bacon, A. A. Hasapis, and J. W. Wholley, Jr., "Viscosity and Density of Molten Silica and High Silica Content Glasses," Phys. and Chem. of Glasses 1, 90-98 (1960).

18. J. C. Rowley, LASL, Private Communication, April 1972.

19. J. F. Bacon, S. Russell and J. P. Carstens, "Determination of Rock Thermal Properties," United Aircraft Research Laboratories Report AD-755218 (January 1973).

20. J. D. Mackenzie, Trans. Faraday Soc. 52, 1564 (1956).

21. H. R. Shaw, "Rheology of Basalt in Melting Range," J. Petrology 10, 510 (1969).

22. S. P. Clark, Jr., (Ed.), Handbook of Physical Constants, Geol. Soc. of Amer., Mem. 97, New York (1966).

23. E. B. Allison, P. Brock and J. White, "The Rheology of Aggregates Containing a Liquid Phase with Special Reference to the Mechanical Properties of Ceramics at High Temperatures," Trans. British Ceram. Soc. 58, 495-531 (1959).

24. K. L. Loewenstein, The Manufacturing Technology of Continuous Glass Fibres, Elsevier Scientific Publishing Co., Amsterdam (1973).

25. H. Bloom and J. O'M. Bockris, "Molten Electrolytes," in Modern Aspects of Electrochemistry, Vol. 2, J. O'M. Bockris (Ed.) Academic Press, NY (1959).

26. D. C. Presnall, C. L. Simmons and H. Porath, "Changes in Electrical Conductivity of a Synthetic Basalt During Melting," J. of Geophys. Res. 77, 5665-5672 (1972).

27. T. Murase, "Viscosity and Related Properties of Volcanic Rocks at 800 to 1400°C," J. Fac. Sci. Hokkaido Univ., Ser. 7, 1, 487-584 (1962).

28. T. Nagata, "Some Physical Properties of the Lava of Volcanoes Asama and Mihara," Bull. Earthquake Res. Inst. 15, 663-673 (1937).

29. M. P. Valorovich and D. M. Tolstoi, "The Simultaneous Measurement of Viscosity and Electrical Conductivity of Some Fused Silicates at Temperatures up to 1400°C," Soc. Glass Tech. J. 20, 54-60 (1936).

30. H. P. Coster, "The Electrical Conductivity of Rocks at High Temperatures," Geophys. J. Roy. Astron. Soc. 5, 193-199 (1948).

31. E. I. Parkhomenko, Electrical Properties of Rocks, (Plenum, New York, 1967), translated from Russian, 314 pp.

32. A. Stanton, "Heat Transfer and Thermal Treatment Processes in Subterrene-Produced Glass Hole Linings," Los Alamos Scientific Laboratory Report LA-5502-MS, (February 1974).

33. C. L. Babcock, "Viscosity and Electrical Conductivity of Molten Glasses," J. Am. Ceram. Soc. 17, 329-342 (1934).

34. H. R. Lillie, "The Measurement of Absolute Viscosity by the Use of Concentric Cylinders," J. Am. Ceram. Soc. 12, 505 (1929).